Highly Ordered Supermicroporous Silica

Renliang Wang,[†] Shuhua Han,*[,†] Wanguo Hou,[†] Lixin Sun,[†] Jun Zhao,[†] and Youshao Wang[‡]

Key Lab of Colloid and Interface Chemistry (Shandong University) Ministry of Education, Shandong University, Jinan, 250100, P. R. China, and South China Sea Institute of Oceanology, Chinese Academy of Sciences, Guangzhou 510301, P. R. China

Received: February 27, 2007; In Final Form: May 20, 2007

Highly ordered supermicroporous silica (space group 2D-*p*6*mm*) was prepared using gemini surfactant $[C_8H_{17}-N^+(CH_3)_2-(CH_2)_2-N^+(CH_3)_2-C_8H_{17}]\cdot 2Br^-$ (denoted C_{8-2-8}) with a short spacer group ($s = 2$) as the structure-directing agent and sodium silicate as the precursor. The samples were characterized by small-angle X-ray diffraction, transmission electron microscopy, and N_2 adsorption−desorption. The results showed that the pore structure of the resulting silica belongs to the two-dimensional hexagonal structure (space group 2D-*p*6*mm*) with a pore size of ca. 1.40 nm (in the supermicroporous range). The high-quality supermicroporous silica was formed at a low molar ratio of C_{8-2-8} to sodium silicate (0.08:1), indicating that the ability of self-assembly of C_{8-2-8} is stronger than that of corresponding monovalent surfactants (single chain, single head group). For supermicroporous materials, the methods for calculating surface area and pore size are critically compared. The surface area was found to be about 1000 m^2/g by the α_s plot method. The pore size obtained with the HK model was in the range of 1.36−1.62 nm.

Introduction

The pore diameters of supermicroporous materials are in the range of 1−2 nm, which is larger than those of conventional zeolites (diameter < 1 nm) but smaller than those of mesoporous materials (diameter ≈ 2−50 nm). Since 1992, ordered mesoporous materials such as M41S,[1,2] SBA,[3−5] MSU,[6] and HMM[7] have been synthesized using supramolecular templates. The pore size of ordered mesoporous silica can be controlled by choosing surfactants with different carbon chain lengths, and the smallest pore size obtained was about 2 nm. As a catalyst carrier, however, the pore size of ordered mesoporous silica is too large to show shape- and size-selective properties in catalyzed reactions. Therefore, the synthesis of supermicroporous materials with pore diameters falling between those of zeolites and mesoporous materials is an interesting topic in the fields of separation and catalysis.[8−12]

Compared to ordered mesoporous materials, the synthetic methods and properties of ordered supermicroporous materials have seldom been reported. Zhao et al.[13] reported a method in which tetraethylorthosilicate was deposited in as-synthesized MCM-41 and then hydrolyzed for tailoring the pore-opening sizes of MCM-41 materials. Supermicroporous aluminosilicates[14−16] and niobium phosphates[17] have been synthesized using primary amines or alkyltrimethylammonium bromide ($n = 10$, 12, 16). Bagshaw et al.[18,19] synthesized supermicroporous silica (1.6−2.0 nm) using micelles of bola-form surfactants in which the molar ratio of SiO_2 to the surfactant dominated the pore structure of the resulting silica. Supermicroporous organic-integrated silica[20] and pure silica[21] have been synthesized in such mixed surfactants as alkylamine/alkyl(phenyl)polyethylene oxide and mixtures of short double-chain alkylammmonium surfactants, among others. Recently, highly ordered monolithic supermicroporous lamellar silica has been prepared in room-temperature ionic liquids by the nanocasting technique.[22,23] Thermally stable supermicroporous silica has been synthesized using hydrated α-sodium disilicate as a precursor.[24] Ordered hexagonal smaller supermicroporous silica has been synthesized in a surfactant/co-surfactant system[25] or at ultralow temperature using semifluorinated surfactants.[26]

In this article, the gemini surfactant $[C_8H_{17}N^+(CH_3)_2-(CH_2)_2-N^+(CH_3)_2C_8H_{17}]\cdot 2Br^-$ (denoted C_{8-2-8},) was used to synthesize highly ordered supermicroporous silica through the S^+I^- routine (sodium silica as precursor). Gemini surfactants[27,28] are a relatively new class of amphiphilic molecules containing two head groups and two aliphatic-chains, linked by a spacer group. By varying the lengths of the spacer group and alkyl chains, different molecular structures of gemini surfactants can easily be obtained. Compared to the corresponding monovalent surfactants (single chain, single head group), gemini surfactants have some unique characteristics, such as high surface activities, strong self-assembly abilities, and special rheologic behaviors. Thus, gemini surfactants have potential applications in skin care, antibacterial materials, construction of porous materials, analytical separations, and solubilization processes.

Some articles have been published on the synthesis of mesoporous materials templated by gemini surfactants. Huo et al.[4] synthesized MCM-41 (2D hexagonal *P*6*mm*), MCM-48 (cubic *Ia*3*d*), and MCM-50 (lamellar) using gemini surfactants with different spacer lengths ($C_{16-s-16}$, $s = 2-12$). Van Der Voort et al.[29] synthesized MCM-41 and MCM-48 using gemini surfactants $C_{16-8-16}$ and C_{n-s-n} ($n = 16$, 18, 22; $s = 10$, 12), respectively. Widenmeyer et al.[30] reported pore size control of mesostructure silica using mixtures of gemini surfactants, via hydrothermal restructuring. Later, gemini surfactants with short spacers C_{n-2-n} ($n = 12$, 14)[31,32] were used to synthesize cubic *Ia*3*d* ($n = 12$) and *Pm*3*n* ($n = 14$). Shen et al.[33] synthesized mesoporous silica with a 3D cubic mesostructure (space group *Fd*3*m*) using the cationic surfactant $C_{n-2-3-1}$ ($n = 14$, 16, 18).

* To whom correspondence should be addressed. E-mail: shuhhan@sdu.edu.cn.
[†] Shandong University.
[‡] Chinese Academy of Sciences.

10.1021/jp0716029 CCC: $37.00
Published on Web 06/30/2007

These results show that use of gemini surfactants as structure-directing agents is conducive to the understanding of the relationship between the structure-directing agent and the final mesostructure and of the effect of the surfactant self-assembly ability on the ordering of mesostructure materials. To date, the synthesis of supermicroporous silica using gemini surfactants as structure-directing agents has not been reported.

Experimental Section

1. Reagents. C_{8-2-8} gemini surfactant was synthesized according to the literature method.[34] The critical micelle concentration of C_{8-2-8} is 21.1 mmol/L (25 °C), and the lowest point did not occur in the curve of surface tension vs concentration of the surfactant, indicating that C_{8-2-8} was pure.

Crystalline sodium silicate, with 21.05% (w/w) Na_2O and a Na_2O-to-SiO_2 molar ratio of 1.03, was obtained from Shanghai Fourth Reagent Plant. Sulfuric acid (98%) was an analytical-grade reagent obtained from Zhangzhou Second Regent Plant.

2. Synthesis. In a typical procedure for the synthesis of supermicroporous silica, an appropriate amount of C_{8-2-8} and 1.71 g of $Na_2SiO_3 \cdot 9H_2O$ were first dissolved in 29.0 mL of distilled water, and then the surfactant solution and sodium silicate solution were rapidly mixed with stirring at room temperature. Twenty minutes later, 2 mol/L sulfuric acid solution was quickly added with vigorous stirring. (The molar composition of the gel was 1 Na_2SiO_3/0.04−2.22 C_{8-2-8}/550 H_2O.) After 5 min, precipitate formed, and the solution was allowed to stand at room temperature for 5 h. The reaction mixture was then kept at a hydrothermal temperature of 80 °C for 3 days in a heating box. (The final pH value of the mixture was in the range of 8−9.) The resulting samples were recovered by filtration, washed with distilled water, and dried at room temperature. The surfactants were removed by calcination at 550 °C for 6 h in air.

3. Characterization. Powder small-angle X-ray diffraction data were obtained on a D/max-rB model instrument operating at low angle (2θ from 1° to 10°) with a Cu target at 40 kV and 100 mA, using a speed of 2°/min and a step of 0.01°.

TEM images were recorded using a JEOL JEM 2010F electron microscope, operating at 200 kV. The samples were crushed in an agate mortar, dispersed in ethanol, and deposited on a microgrid.

Nitrogen adsorption−desorption isotherms of the materials were determined at −196 °C using a conventional volumetric technique with a Coulter Omnisorp 100CX sorption analyzer. Each sample was degassed at 350 °C for 6 h under a pressure of 10^{-5} Pa or below. The surface area (S_{BET}) was calculated using the BET method. The total pore volume (V_t) was calculated from the amount adsorbed at a relative pressure (P/P_0) of about 0.99. The total surface area (S_t), external surface area (S_{ex}), primary porous surface area (S_p), primary pore volume (V_p), and micropore volume (V_{mi}) were obtained using the α_s plot method.[35−37] S_{ex} was defined as the sum of the surface area of macropores and secondary pores. Li-Chrospher Si-1000 silica gel ($S_{BET} = 25$ m^2/g) was used as a reference adsorbent in the α_s plot analysis.[38] The pore size distribution (PSD) was evaluated using the Barrett−Joyner−Halenda (BJH) and Horvath−Kawazoe (HK) models. Also, the pore size was evaluated using the equation[39]

$$D_d = cd_{100}\left(\frac{\rho V_p}{1+\rho V_p}\right)^{1/2} \quad (1)$$

where ρ is the pore wall density, assumed to be equal to that of amorphous silica density (2.2 g cm^{-3}); c is a constant, depending on the pore geometry ($c = 1.213$ for cylindrical pores); d_{100} is the interlayer distance of the (100) diffraction peak; and V_p is the primary pore volume. The D_{HK} and D_{BJHads} primary pore sizes were defined as the maxima on the PSD.

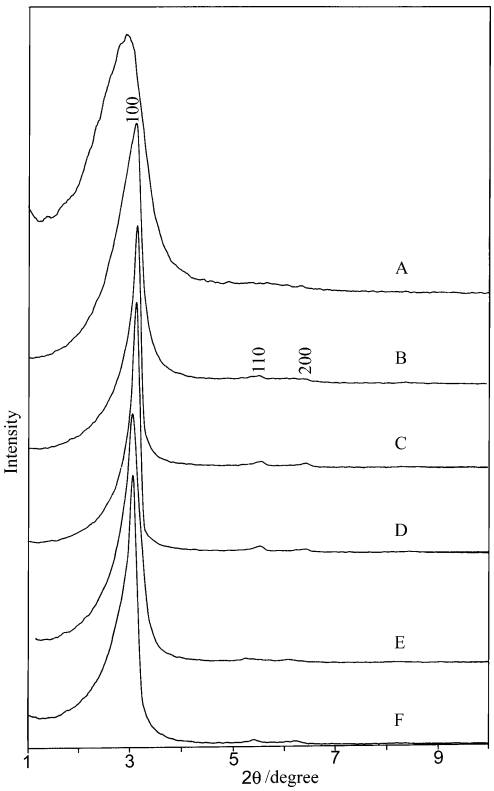

Figure 1. Effect of the molar ratio (x value) of C_{8-2-8} to sodium silicate on the structure of silica: (A) 0.04:1, (B) 0.08:1, (C) 0.111:1, (D) 0.33:1, (E) 1.33:1, (F) 2.22:1).

Results and Discussion

The X-ray diffraction (XRD) patterns of the samples are shown in Figure 1. From these patterns, we can see only one diffraction peak at a molar ratio of C_{8-2-8} to sodium silicate (x value) of 0.04:1. With increasing x value from 0.08:1 to 2.22:1, three diffraction peaks appear, indexed as (100), (110), and (200) in the as-synthesized samples. These peaks were attributed to the two-dimensional hexagonal lattice symmetry (space group 2D-$p6mm$). The appearance of the (110) and (200) diffraction peaks in the as-synthesized samples indicates that the porous structure was more ordered. These results are quite different from those obtained using octanetrimethylammonium bromide (C_8TMA) as the structure-directing agent.[40] First, only one small and broad diffraction peak appeared in the XRD pattern, indicating that a less-order pore structure was obtained using C_8TMA as the structure-directing agent. Second, the concentrations of the structure-directing agents were quite different; for C_8TMA, the concentration was about 11 wt %, whereas for C_{8-2-8}, it was 0.36 wt %; obviously, the latter is much lower than the former. These results show that the self-assembly ability and the ordering of the pore structure are higher for gemini surfactant C_{8-2-8} than for C_8TMA.

The unit cell constants, a values (pore-center distance between two adjacent pores, calculated as $a = 2d_{100}/3^{1/2}$), and d_{100} values are listed in Table 1. As can be seen from Table 1, the pore-center distance (a_0) between two adjacent pores of silica was about 3.2 nm, which seemed not to be obviously affected by

TABLE 1: Effect of the Molar Ratio of C_{8-2-8} to Sodium Silicate (*x* Value) on the Surface Properties of Silica

x value	d_{100} (nm)	a_0 (nm)	S_{BET} (m^2/g)	S_t (m^2/g)	S_p (m^2/g)	S_{ex} (m^2/g)	V_t (cm^3/g)	V_p (cm^3/g)	D_d (nm)	D_{BJHads} (nm)	D_{HK} (nm)
0.04:1	2.97	3.43	345	366	316	50	0.21	0.13	–	–	–
0.08:1	2.79	3.22	1262	920	839	81	0.52	0.42	2.34	1.35	1.44
0.11:1	2.76	3.19	1344	968	897	71	0.55	0.46	2.37	1.36	1.43
0.33:1	2.78	3.21	1338	1043	973	70	0.54	0.46	2.39	1.30	1.36
1.33:1	2.80	3.23	1402	1049	967	82	0.65	0.45	2.39	1.53	1.62
2.22:1	2.84	3.28	1336	1000	923	77	0.67	0.50	2.49	1.49	1.57

the *x* value. Figure 2 shows the pore structure along the hexagonal [110] plane; the silica walls (ca. 1.5 nm) were perfectly parallel to each other. The pore size was about 1.2 nm. The corresponding Fourier diffractogram displays first-, second- and third-order spot patterns, indicating that the supermicropore array was a highly ordered crystal-like structure.

Type IV adsorption isotherms[41] for the above supermicroporous materials are shown in Figure 3. Over a P/P_0 range of 0.04−0.1 Pa, steplike curves appeared as a result of capillary condensation in the resulting samples. Compared to those of mesoporous silica, the position of the steplike curves shifted to lower P/P_0 values, indicating that small pores existed in the resulting sample. The adsorption and desorption curves coincided, and no hysteresis loop appeared in the whole range of P/P_0 examined, showing that the pore channels were uniform, i.e., monodisperse pores existed in the resulting samples. Also, the height of the steplike curves gradually increased with increasing *x* value.

The specific surface area was generally obtained using the BET method in the P/P_0 range of 0.05−0.30; however, the range of P/P_0 values used for calculating the BET surface areas of the supermicropore samples must be reset. BET plots are shown in Supporting Information Figure 1S; a linear range was found between 0.04 and 0.12 P/P_0. When P/P_0 was higher than 0.12, a deviation from linearity was observed. Thus, the P/P_0 range of 0.04−0.12 was selected to calculate the BET surface areas (S_{BET}). The α_s plot method (Supporting Information Figures 2S−8S) can also be used to evaluate the surface area (here defined as the total surface area, S_t). S_{BET} and S_t values are listed in Table 1. As can be seen from Table 1, the S_{BET} values are larger than those of the S_t values; this result was ascribed to condensation of nitrogen in primary supermicropores, which leads to overestimation of the specific surface area from the BET method. S_p and V_p were in the range of 839−973 m^2/g and 0.42−0.50 cm^3/g, respectively, and they constituted about 91−93% of S_t and 69−85% of V_t, respectively, The above results indicate that the primary pores, i.e., supermicropores, are in a great majority in the resulting samples.

PSDs were calculated from nitrogen adsorption data using the HK (Figure 4), BJH (Supporting Information Figure 8S), and geometrical models. The primary pore sizes D_{HK}, D_{BJHads}, and D_d are listed in Table 1. As can be seen from Table 1, D_{HK}, D_{BJHads} and D_d were ca. 1.44, 1.35, and 2.37 nm, respectively, i.e., $D_d > D_{HK} > D_{BJHads}$. According to the previous method of calculating pore sizes, which is based on the length of the alkyl chain of the gemini surfactant C_{8-2-8},[31] the pore size was 1.78 nm, i.e., the maximum pore size value in the supermicroporous silica. If the framework shrinkage of supermicroporous silica caused by calcination is considered, the pore size obtained by the HK diameter model is reasonable and close to the value obtained by TEM (1.2 nm). The geometrical model can overestimate the pore size through the use of the bulk silica density in calculating the pore size according to eq 1, whereas the BJH model can underestimate the pore size through the overestimation of the transition pressures caused by the effect of the capillary force on the amount of nitrogen adsorbed when the pore size is below 2 nm.[42] These conclusions are consistent with those of Kruk et al.[39,43]

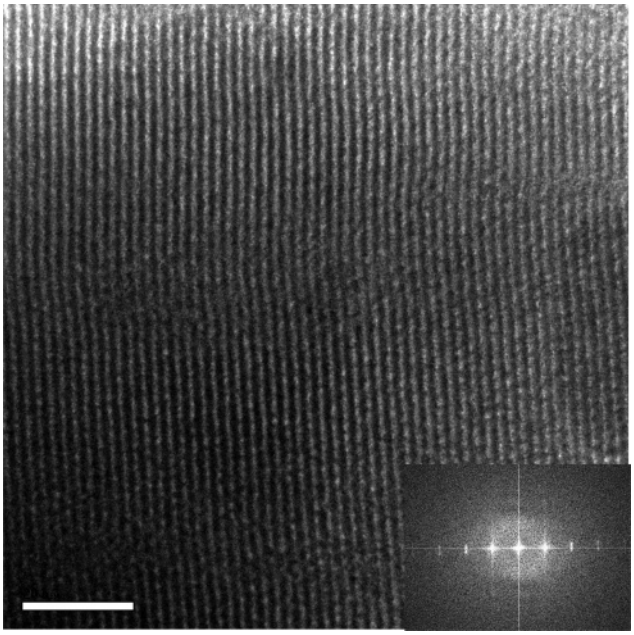

Figure 2. HRTEM image of the sample with an *x* value of 0.11:1. The length of the white scale bar is 20 nm. The inset is the corresponding Fourier diffraction pattern.

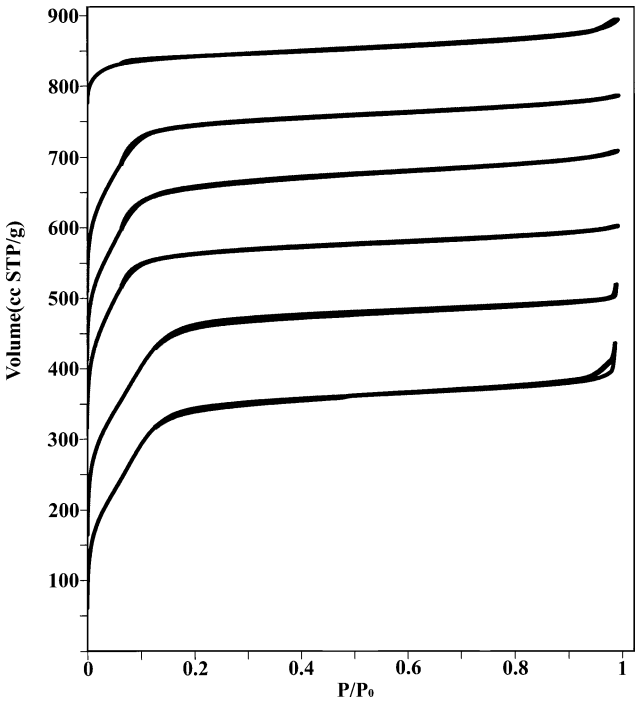

Figure 3. N_2 adsorption−desorption isotherms at −196 °C of the calcined samples at different *x* values. From top to bottom: 0.04:1, 0.08:1, 0.111:1, 0.33:1, 1.33:1, 2.22:1.

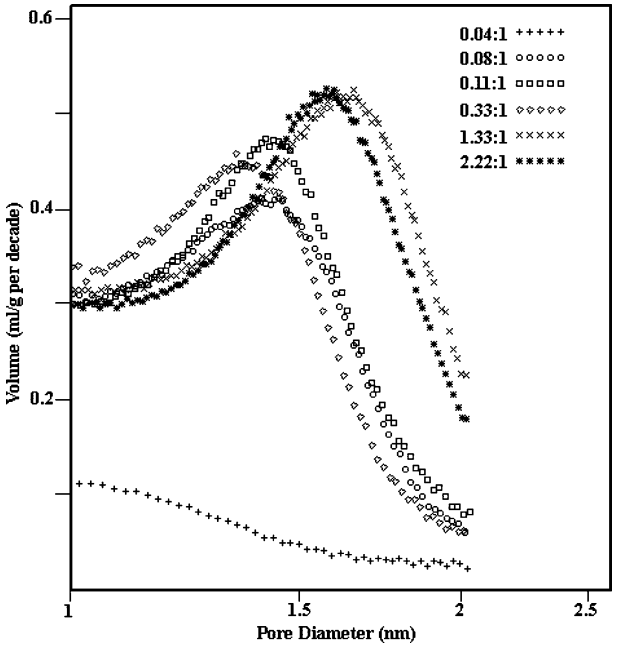

Figure 4. Pore size distribution curves obtained with the HK model for calcined samples with different *x* values (calculated from adsorption data).

Conclusion

Under mild conditions, highly ordered supermicroporous silica materials (2D-*p*6*mm*) have been synthesized using a gemini surfactant with a short spacer of $s = 2$ (C_{8-2-8}) as the structure-directing agent and sodium silicate as the precursor. The ordering of the pore structure increased with increasing *x* value (molar ratio of C_{8-2-8} to sodium silicate).

Type IV adsorption−desorption isotherms and no hysteresis loops were observed in the N_2 adsorption−desorption curves. For supermicroporous materials, the methods of calculating surface area and pore size were critically compared. The surface area was about 1000 m^2/g by the α_s plot method. The pore size obtained by the HK model was in the range of 1.36−1.62 nm.

Acknowledgment. This research was financially supported by the Key Project Foundation of the Ministry of Education of China (No. 105104), the Natural Science Foundation of China (No. 50572057), the Middle-aged and Youthful Excellent Scientist Encouragement Foundation of Shandong (No. 2005BS1-1003), and the Natural Science Foundation of Shandong Province (No. Z2006B02).

Supporting Information Available: BET plots, α_s plots, and pore size distribution curves obtained with the BJH model for calcined samples at different molar ratios of C_{8-2-8} to sodium silicate. This material is available free of charge via the Internet at http://pubs.acs.org.

References and Notes

(1) Kresge, C. T.; Leonowicz, M. E.; Roth, W. J.; Vartuli, J. C.; Beck, J. S. *Nature* **1992**, *359*, 710−712.;

(2) Beck, J. S.; Vartuli, J. C.; Roth, W. J.; Leonowicz, M. E.; Kresge, C. T.; Schmitt, K. D.; Chu, C. T-W.; Olson, D. H.; Sheppard, E. W.; McCullen, S. B.; Higgins, J. B.; Schlenker, J. L. *J. Am. Chem. Soc.* **1992**, *114*, 10834−10843.

(3) Huo, Q.; Margolese, D. I.; Ciesla, U.; Feng, P.; Gier, T. E.; Sieger, P.; Leon, R.; Petroff, P. M.; Schüth, F.; Stucky, G. D. *Nature* **1994**, *368*, 317−321.;

(4) Huo, Q.; Margolese, D. I.; Stucky, G. D. *Chem. Mater.* **1996**, *8*, 1147−1160.

(5) Zhao, D.; Huo, Q.; Feng, J.; Chmelka, B. F.; Stucky, G. D. *J. Am. Chem. Soc.* **1998**, *120*, 6024−6036.

(6) Bagshaw, S. A.; Prouzet, E.; Pinnavaia, T. J. *Science* **1995**, *269*, 1242−1244.

(7) Inagaki, S.; Guan, S.; Fukushima, Y.; Ohsuna, T. *J. Am. Chem. Soc.* **1999**, *121*, 9611−9614.

(8) Corma, A.; Rey, F.; Rius, J.; Sabater, M. J.; Valencia, S. *Nature* **2004**, *431*, 287−290.

(9) Shin, Y.; Liu, J.; Wang, L.-Q.; Nie, Z.; Samuels, W. D.; Fryxell, G. E.; Exarhos, G. J. *Angew. Chem., Int. Ed.* **2000**, *39*, 2702−2707;

(10) Christensen, C. H.; Johannsen, K.; Schmidt, I.; Christensen, C. H. *J. Am. Chem. Soc.* **2003**, *125*, 13370−13371.

(11) Svec, F.; Fréchet, J. M. J. *Adv. Mater.* **1994**, *6*, 242−244.

(12) Katiyar, A.; Ji, L.; Smirniotis, P.; Pinto, N. G. *J. Chromatogr. A* **2005**, *1069*, 119−126.

(13) Zhao, X. S.; Lu, G. Q. (Max); Hu, X. *Chem. Commun.* **1999**, 1391−1392.

(14) B.-Gonzalez, E.; Mokaya, R.; Jones, W. *Chem. Commun.* **2001**, 1016−1017.

(15) Serrano, D. P.; Aguado, J.; Escola, J. M.; Garagorri, E. *Chem. Commun.* **2000**, 2041−2042.

(16) Yano, K.; Fukushima, Y. *J. Porous Mater.* **2003**, *10*, 223−229.

(17) Mal, N. K.; Fujiwara, M. *Chem. Commun.* **2002**, 2702−2703.

(18) Bagshaw, S. A.; Hayman, A. R. *Chem. Commun.* **2000**, 533−534.

(19) Bagshaw, S. A.; Hayman, A. R. *Adv. Mater.* **2001**, *13*, 1011−1013.

(20) McInall, M. D.; Scott, J.; Mercier, L.; Kooyman, P. J. *Chem. Commun.* **2001**, 2282−2283.

(21) Ryoo, R.; Park, I.-S.; Jun, S.; Lee, C. W.; Kruk, M.; Jaroniee, M. *J. Am. Chem. Soc.* **2001**, *123*, 1650−1657.

(22) Zhou, Y.; Antonietti, M. *Adv. Mater.* **2003**, *15*, 1442−1455.

(23) Zhou, Y.; Antonietti, M. *Chem. Mater.* **2004**, *16*, 544−550.

(24) Kato, M.; Shigeno, T.; Kimura, T.; Kuroda, K. *Chem. Mater.* **2005**, *17*, 6416−6421.

(25) Lin, Y.-S.; Lin, H.-P.; Mou, C.-Y. *Microporous Mesoporous Mater.* **2004**, *76*, 203−208.

(26) Di, Y.; Meng, X.; Wang, L.; Li, S.; Xiao, F.-S. *Langmuir* **2006**, *22*, 3068−3072.

(27) Zana, R. *Adv. Colloid Interface Sci.* **2002**, *97*, 205−253.

(28) Menger, F. M.; Keiper, J. S. *Angew. Chem., Int. Ed.* **2000**, *39*, 1906−1920.

(29) Van Der Voort, P.; Mathieu, M.; Mees, F.; Vansant, E. F. *J. Phys. Chem. B* **1998**, *102*, 8847−8851.

(30) Widenmeyer, M.; Anwander, R. *Chem. Mater.* **2002**, *14*, 1827−1831.

(31) Han, S.; Xu, J.; Hou, W.; Yu, X. M.; Wang, Y. S. *J. Phys. Chem. B* **2004**, *108*, 15043−15048.

(32) Han, S.; Hou, W.; Xu, J.; Huang, X.; Zheng, L. *ChemPhysChem* **2006**, *7*, 394−399.

(33) Shen, S. D.; Li, Y. Q.; Zhang, Z. D.; Fan, J.; Tu, B.; Zhou, W. Z.; Zhao, D. Y. *Chem. Commun.* **2002**, 2212.

(34) Zana, R.; Benrraou, M.; Rueff, R. *Langmuir* **1991**, *7*, 1072−1075.

(35) Kruk, M.; Jaroniec, M.; Kim, J. M.; Ryoo, R. *Langmuir* **1999**, *15*, 5279−5284.

(36) Qiao, S. Z.; Bhatia, S. K.; Zhao, X. S. *Microporous Mesoporous Mater.* **2003**, *65*, 287−298.

(37) Rathouský, J.; Schulz-Ekloff, G.; Zukal, A. *Microporous Mater.* **1996**, *6*, 385−394.

(38) Jaroniec, M.; Kruk, M.; Olivier, J. P. *Langmuir* **1999**, *15*, 5410−5413.

(39) Kruk, M.; Jaroniec, M.; Sayari, A. *J. Phys. Chem. B* **1997**, *101*, 583−589.

(40) Beck, J. S.; Vartuli, J. C.; Kennedy, G. J.; Kresge, C. T.; Roth, W. J.; Schramm, S. E. *Chem. Mater.* **1994**, *6*, 1816−1821.

(41) Sing, K. S. W.; Everett, D. H.; Haul, R. A. W.; Moscou, L.; Pierotti, R. A.; Rouquerol, J.; Siemieniewska, T. *Pure Appl. Chem.* **1985**, *57*, 603−619.

(42) Ravikovitch, P. I.; Domhnaill, S. C. Ó; Neimark, A. V.; Schuth, F.; Ungert, K. K. *Langmuir* **1995**, *11*, 4765−4772.

(43) Kruk, M.; Jaroniec, M.; Sayari, A. *Langmuir* **1997**, *13*, 6267−6273.